Biomedical Signal Processing and Control 18 (2015) 161–168

Contents lists available at ScienceDirect

Biomedical Signal Processing and Control

journal homepage: www.elsevier.com/locate/bspc

Segmentation of overlapping *Cryptosporidium* and *Giardia* (oo)cysts using bidirectional contour tracing

Shahriar Badsha [a], Hamzah Arof [a,*], Norrima Mokhtar [a], Yvonne Ai Lian Lim [b], Marizan Mubin [a], Mahazani Mohamad [a]

[a] Department of Electrical Engineering, Faculty of Engineering, University of Malaya, 50603 Kuala Lumpur, Malaysia
[b] Department of Parasitology, University of Malaya, 50603 Kuala Lumpur, Malaysia

ARTICLE INFO

Article history:
Received 22 September 2014
Received in revised form
16 November 2014
Accepted 10 December 2014
Available online 24 January 2015

Keywords:
Contour tracing
Ellipse segmentation

ABSTRACT

In the inspection of treated water samples under microscope, knowing the average number of parasite (oo)cysts like *Giardia* and *Cryptosporidium* that exist in the samples is crucial as it tells whether the water is safe for consumption. Here, we introduce a new approach using a bidirectional contour tracing technique to segment and enumerate overlapping *Cryptosporidium* and *Giardia* (oo)cysts in microscopic images of treated water samples. First the image is denoised and edge detection is performed to detect the boundary of the (oo)cysts using Kirsch operator. The greyscale image is then binarized to identify the position of the (oo)cysts before it is Otsu thresholded to separate weak edge from strong edge. Then bidirectional contour tracing is implemented to isolate overlapping objects where the boundary of the (oo)cysts is traced in two different directions simultaneously. After boundary tracing, a modified ellipse fitting is executed where partial or broken ellipses can be combined to form completed ellipses that represent (oo)cysts. The proposed technique is tested on 40 FITC microscopic images containing overlapping *Cryptosporidium* and *Giardia* (oo)cysts in treated water samples. The performance of the technique is comparable to better than those of four well-known ellipse detection methods. The technique is also tested on images containing overlapping blood cells, *Cryptosporidium* oocysts in dirty background and rice grains, and the results are excellent.

1. Introduction

Object recognition is an active area of research in image analysis and computer vision. The detection of elliptical objects in images is important since many natural objects like human face, eyes and fruits are elliptical to a certain extent. In fact, circles can be regarded as a special case of an ellipse. Practical applications of ellipse detection in images are not limited for inspection of rigid industrial parts such as washers, rings, and plates, but also for identification of non-rigid objects such as parasites, facial features, erythrocyte and others. Various ellipse detection techniques and applications have been published in the literature but applying contour tracing and ellipse fitting to segment and count overlapping *Cryptosporidium* and *Giardia* (oo)cysts in treated water samples has not been reported yet to the best of our knowledge.

Since its inception, Hough transform (HT) has been one of the most widely used techniques for detecting lines, ellipses and circles. Many derivatives of the classical HT have been introduced specifically to improve its efficiency in ellipse detection. Methods like adaptive HT by Illingworth [1], generalized HT by Ballard [2], randomized HT by Xu et al. [3], dynamic HT by Xie and Ji [4], restricted randomized HT by Cheng and Liu [5], fast graphical ellipse detection (FGED) by Elmowafy and Fairhurst [6] and multipass Hough transform with pyramid image structure by Chien and Cheng [7], have been proposed to reduce the amount of computations and memory requirement while enhancing its accuracy.

Genetic algorithm (GA) based ellipse detection techniques are slightly different than the HT in implementation but similar in philosophy. They also use edge pixels on the ellipse contour to calculate and subsequently maximize the fitness of the ellipse [8]. Variations of the GA method for ellipse detection have also been introduced to reduce computation and increase its efficiency and robustness. Examples of improved genetic algorithm methods are Multi Population Genetic Algorithm (MPGA) by Yao, Kharma and Grogono [9],

* Corresponding author. Tel.: +60 3 79674456.
E-mail addresses: seul.cse@gmail.com (S. Badsha), ahamzah@um.edu.my (H. Arof), norrimamokhtar@um.edu.my (N. Mokhtar), limailian@um.edu.my (Y.A.L. Lim), marizan@um.edu.my (M. Mubin), mahazani@um.edu.my (M. Mohamad).

http://dx.doi.org/10.1016/j.bspc.2014.12.009
1746-8094/

Table 1
Summary of well-known ellipse detection methods.

Author	Method	Description	Detecting overlapping objects	Object type
Illingworth et al.	Adaptive HT	Detection of 2-D shapes using small accumulator array	No	Rigid
Ballard et al.	Generalized HT	Using the boundary of arbitrary shape to map between image space and HT	No	Rigid
Lei et al.	Randomized HT	Curve detection	No	Rigid
Xie et al.	Dynamic HT	Takes the advantage of major axis	Yes	Rigid
Cheng et al.	Restricted randomized HT	Restrict the scope of selected points when detecting ellipses	Yes	Non-rigid
Elmowafy et al.	FGED	Overcome the substantial time and storage requirements associated with common voting algorithms	Yes	Non-rigid
Chien et al.	Multipass HT	Searching ellipses from lower to higher resolution in multipass fashion	No	Rigid
Lutton et al.	Genetic algorithm to detect 2-D geometric primitives	Efficient approach to search in a high dimensional space	Yes	Rigid
Yao et al.	MPGA for robust ellipse detection	Utilizes both evolution and clustering to direct the search for ellipses – full or partial	Yes	Non-rigid
Chung-Fang et al.	Robust ellipse detection	The approach is based on a multipass Hough transform and an image pyramid data structure	Yes	Rigid

Genetic Algorithm with penalty by Mainzer [10] and Genetic Algorithm with fitness tuning by Lutton and Martinez [8]. The summary of some well-known ellipse detection methods discussed is listed in Table 1.

Contour tracing is mainly used for simple object boundary detection and shape classification. Vaddi and Anne [11] proposed an approach for object detection by finding its contour using freeman chain code which is similar to contour tracing. Chang and Chen [12] introduced an algorithm that uses a contour tracing technique to detect the external contour and possible internal contours of objects in binary images. They claimed that their algorithm not only labels components but also extracts component contours and the orders of contour points. Wagenknecht [13] presented a contour tracing and coding algorithm for generating optimized 2D contours from 3D classified objects. Unlike the common pixel-based contour tracing method, the presented method can take into account single pixels and furcation. An ontological representation on coupling active contours was presented in order to understand the scene of multiple non-rigid objects from moving camera. Olszewska and Mccluskey developed an ontology-coupled active contours for dynamic video scene tracking and segmentation by analyzing the object shape and color [14]. The proposed technique in this paper models the *Cryptosporidium* and *Giardia* (oo)cysts as elliptical objects. Edge pixels on the contour of the parasites are detected and evaluated before they are connected together to form an object using contour tracing technique. Then each contour is subjected to certain conditions such as size and square error to certify it as an ellipse before counting. The rest of the paper is organized as follows. In the next section, the methodology of the proposed approach is presented. Steps that are involved in the approach are explained in detail. This is followed by the experimental result section where the performance of the proposed method is discussed and then compared to those of four other methods. Finally, conclusion is drawn and suggestions for future work are given.

2. Methodology

The proposed algorithm consists of three major steps which are pre-processing, contour detection and ellipse segmentation. In the pre-processing part greyscale conversion, filtering, edge detection and thresholding are performed. This is followed by contour detection step wherein binarization and morphological operations are implemented before contour tracing to detect the outline of the (oo)cysts in the image. In the last step, the contours of overlapping (oo)cysts are segmented and an ellipse is fitted in each of them. Fig. 1 shows the flowchart of the proposed algorithm.

2.1. Preprocessing

After greyscale conversion, the input image $I(x, y)$ is filtered to remove noise while preserving edge. Edge preservation is important so that individual (oo)cysts can be identified and segmented properly. A modified fourth order PDE diffusion filter is chosen where the energy function is minimized as follows [15]:

$$E(I) = \int_{\Omega} f(|\nabla^2 I|)\partial\Omega \tag{1}$$

where $E(I)$ is the energy function, $|\nabla^2 I|$ is the magnitude of the Laplacian of I and Ω is the support domain in the image (I). The global minimum of $f(|\nabla^2 I|)$ is at $|\nabla^2 I|$=0. The minimization of the energy function is equivalent to smoothing the image to piecewise planar. The corresponding Euler equation for the energy function is

$$\nabla^2(c(|\nabla^2 I|)\nabla^2 I) = 0 \tag{2}$$

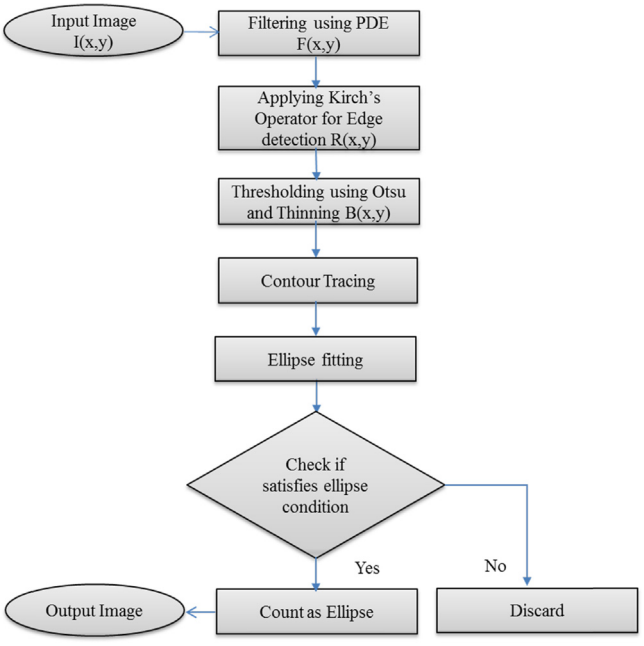

Fig. 1. Flow chart of proposed methodology.

5	-3	-3	5	5	-3	5	5	5	-3	5	5	-3	-3	-3	-3	-3	-3	-3	-3
5	0	-3	5	0	-3	-3	0	-3	-3	0	5	-3	0	-3	-3	0	5	5	0
5	-3	-3	-3	-3	-3	-3	-3	-3	-3	-3	-3	-3	-3	-3	5	5	-3	5	5

Fig. 2. Kirsch operator.

and it can be solved through gradient descent procedure as

$$\frac{\partial I}{\partial t} = \nabla^2(c(|\nabla^2 I|)\nabla^2 I) \tag{3}$$

where the diffusion coefficient is

$$c(\nabla^2 I) = \frac{f'(|\nabla^2 I|)}{|\nabla^2 I|} \tag{4}$$

In this work, the diffusion coefficient is replaced by

$$c(O_k I) = \frac{1}{1 + (O_k I/z)^2} \tag{5}$$

and the PDE becomes

$$\frac{\partial I}{\partial t} = \nabla^2(c(|O_k I|)O_k I) \tag{6}$$

where $O_k I$ represents the convolution of a rotated 3×3 Prewitt operator and image I, k is the index of the rotated Prewitt operator that generates the maximum gradient and $z = 0.5$. The implementation of Eq. (6) is as follows. Each 3×3 neighborhood on image I is convolved with 3×3 Prewitt operator rotated at 0°, 45°, 90°, 135°, 180°, 225°, 270° and 315°. The angle of the operator that produces the maximum absolute convolution value is denoted as k and the convolution outcome, $O_k I$, is taken as the local gradient of the neighborhood. Once $c(O_k I)O_k I$ is computed for the whole image, the discrete Laplacian $\nabla^2 c(O_k I)O_k I$ for the image is calculated using the following formula:

$$\nabla^2 f(x,y) = f(x-1,y) + f(x+1,y) + f(x,y-1) + f(x,y+1) - 4f(x,y) \tag{7}$$

where $f(x,y) = c(O_k I)O_k I(x,y)$.

The output filtered image is called $F(x,y)$. After filtering, edge detection is performed on $F(x,y)$ using rotated Kirsch operators as shown in Fig. 2. Each 3×3 neighborhood in $F(x,y)$ is convolved with the eight operators and the convolution that produces the maximum absolute value is chosen to represent the edge value of the neighborhood. This operation produces an edge image $R(x,y)$ that contains the contours of the (oo)cysts.

Then $R(x,y)$ is Otsu thresholded to separate the weak edge from the strong edge so that spurious weak edge not related to (oo)cysts contour can be removed. Otsu thresholding is chosen since it is designed to group objects into two classes and determines the threshold value, T, automatically.

In principle, Otsu thresholding tries to minimize the total variance of the two classes as follows. Suppose the edge image $R(x,y)$ contains N pixel with grey levels from 1 to L and the number of pixels with grey level i is denoted by g_i. Thus, the probability of grey level i in the image is

$$p_i = \frac{g_i}{N} \tag{8}$$

We wish to group the pixels into two classes, C_1 and C_2 where the grey levels are $[1,\ldots t]$ and $[t+1,\ldots L]$, respectively. If we define the total variance as

$$\sigma^2_{total} = \omega_1(T)\sigma_1^2(T) + \omega_2(T)\sigma_2^2(T) \tag{9}$$

where $\sigma_1^2(T)$ and $\sigma_2^2(T)$ are the variance of the pixels in C_1 (below threshold) and C_2 (above threshold), respectively.

$$\omega_1(t) = \sum_{i=1}^{t} P_i \tag{10}$$

$$\omega_2(t) = \sum_{i=t+1}^{L} P_i \tag{11}$$

Calculating Eq. (9) for all possible T is not trivial. However, there is a simple way of doing it using Otsu method whose details are available in [16]. Once the threshold T is determined, the edge image $R(x,y)$ is converted into a binary image $B(x,y)$ as follows:

$$B(x,y) = \begin{cases} 1 \ \text{(white)} & \text{if } R(x,y) \geq T \\ 0 \ \text{(black)} & \text{if } R(x,y) < T \end{cases} \tag{12}$$

Finally, iterative thinning is performed on $B(x,y)$ to thin the contours of the (oo)cysts until they become chains of pixels with minimum thickness. The resulting image is called $S(x,y)$. Fig. 3 shows the flow of output images until thinning operation.

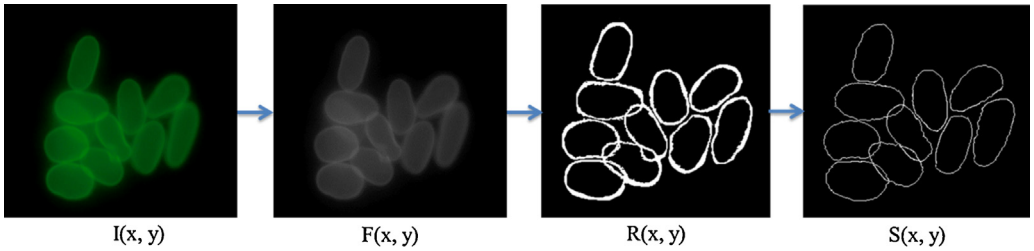

Fig. 3. (From left to right) RGB image, greyscale image, edge image and edge after thinning.

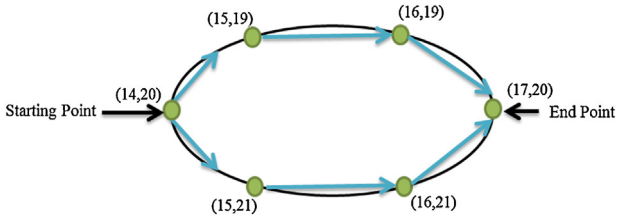

Fig. 4. Contour tracing using two tracing lines.

2.2. Modified contour tracing

A modified contour tracing is used to segment overlapping (oo)cysts modeled as ellipses in $S(x, y)$. The basis of our algorithm is that while moving along the boundary of an (oo)cyst, changes in the direction from one pixel to another should be gradual. In standard contour tracing, the boundary of the object is traversed in one direction. In the modified contour tracing, two tracing lines that run in both clockwise and anti-clockwise directions are used to detect the boundary of an (oo)cyst more quickly and accurately. First, the starting point (pixel) is chosen randomly among the edge pixels. If the starting point is an end point (i.e. the pixel is at the end of a broken ellipse), another starting point is selected. And if the starting point is a junction point (a pixel at the intersection of two or more ellipse boundaries), another starting point is chosen. Junction pixels always appear brighter than other edge pixels and their positions can be identified as follows. First, the locations of edge pixels to be traced in $S(x, y)$ are identified in $F(x, y)$. Then the greyscale values of these pixels in $F(x, y)$ are added and averaged. Finally, the edge pixels in $S(x, y)$ whose greyscale values (in $F(x, y)$) bigger than the average are considered possible junction points.

Then two tracing lines are initiated from the starting pixel in clockwise and anti-clockwise directions as shown in Fig. 4.

The tracing lines advance along the edge pixels of the ellipse boundary simultaneously. All visited edge pixels are recorded, counted and marked so that they will not be re-traced. If any of the tracing lines meets a junction point, it can proceed in more than one direction as shown in Fig. 5. In this situation, it should proceed in the path that least affects its current direction. Thus, at the junction point, the last five pixels of the line are linearized to form a line and its angle with respect to the x axis is calculated. Then the first five consecutive pixels (starting from the junction point) of all possible paths are linearized and their angles calculated. The path whose angle is closest to that of the tracing line is chosen as the path to follow as shown in Fig. 5. If the ellipse is not broken, the two tracing lines should eventually meet at an end point and the ellipse is considered complete.

Table 2
Accuracy of the proposed technique compared to that of the others.

Methods	(oo)cysts detected	Accuracy (%)	Execution time (s)
MPGA	257	96.61	2.02
Young	258	96.99	1.16
FGED	255	96.86	2.51
Chung	254	96.49	1.48
Proposed	262	98.50	1.07

In case the contour is broken, the two tracing lines will not meet and the ellipse is considered incomplete. Both tracing lines will stop at two different endpoints. In this case, the positions of the two endpoints are recorded along with other edge pixels that make up the contour. The length of the partial ellipse is inferred from the number of pixels counted. The pseudocode of the tracing algorithm is given as follows:

```
Initialize data
  Select first starting point randomly
  Record starting point
    Set tracing operator for ellipse as OPC (clockwise) and OPA(anticlockwise)
  While OPC and OPA do not meet do
    Start
      Visit next pixels using OPC, OPA
      if
        OPA or OPC find Junction point
      then
        Visit five consecutive pixel in all paths and calculate their angles
        Record junction point
      Continue tracing along the path with minimum angle
      Record visited pixels
    End while when OPC and OPA meet one another.
  Record endpoint
  End
```

2.3. Ellipse fitting

The *Cryptosporidium* and *Giardia* (oo)cysts are modeled as ellipses. After identifying all (oo)cysts in the image, ellipse fitting is performed on all of them one by one. First, complete ellipses are fitted with conic ellipse model given by Eq. (13) using the coordinates of all the recorded pixels that fall on its contour. Its size is derived from the number of edge pixels that constitute its contour. Ideal contours are drawn using this model and superimposed on the detected ellipses. In the experiments, since the (oo)cysts are nearly identical, the size of the ellipses can be limited to simplify the model when fitting the ellipses and partial ellipses. Partial ellipse fitting starts with the ones with the longest contours. If the end points of two partial ellipses are close together there is a good chance that they can be combined to form one complete ellipse. So a model is fitted to partial ellipses that are in close proximity to see whether

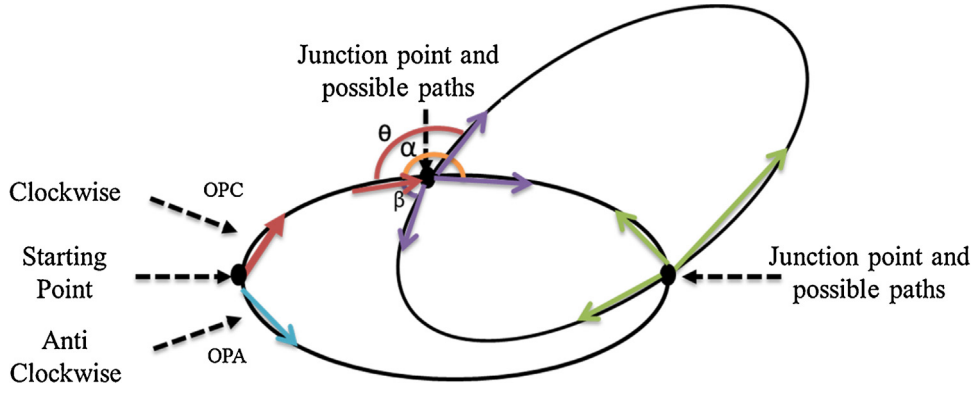

Fig. 5. Finding the right path at junction point (OPC and OPA denotes clockwise and anti-clockwise tracing lines, respectively).

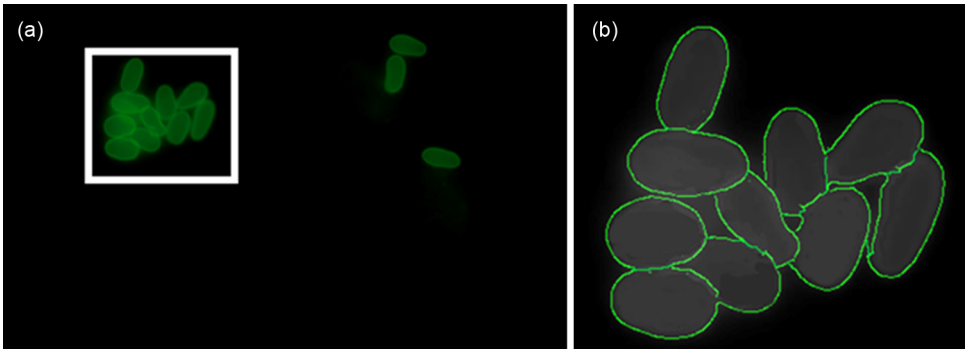

Fig. 6. Detected and segmented parasites (zoomed).

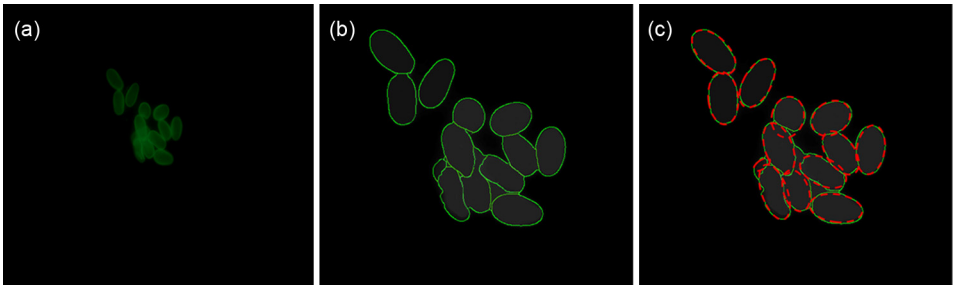

Fig. 7. Sample of image where parasites are not correctly detected: (a) input image, (b) detected parasite, and (c) after ellipse fitting.

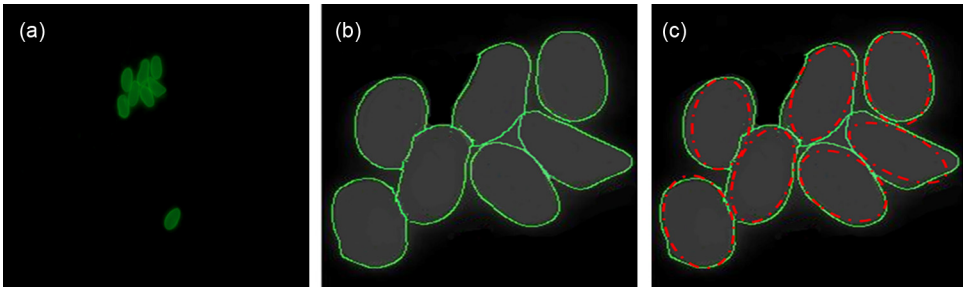

Fig. 8. One sample of image where parasites are detected correctly: (a) input image, (b) detected parasite, and (c) after ellipse fitting.

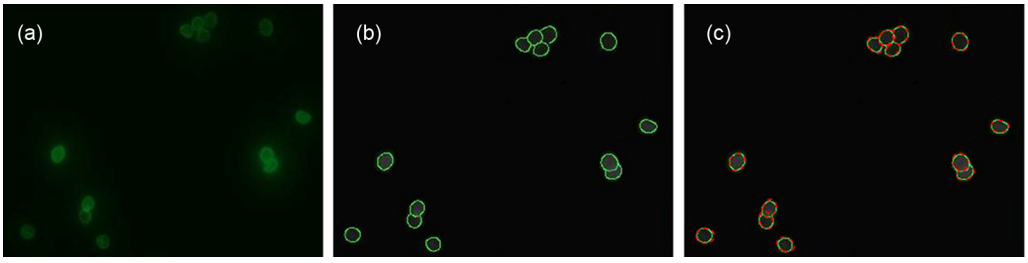

Fig. 9. Sample of *Cryptosporidium* image where parasites are detected correctly: (a) input image, (b) detected parasite, and (c) after ellipse fitting.

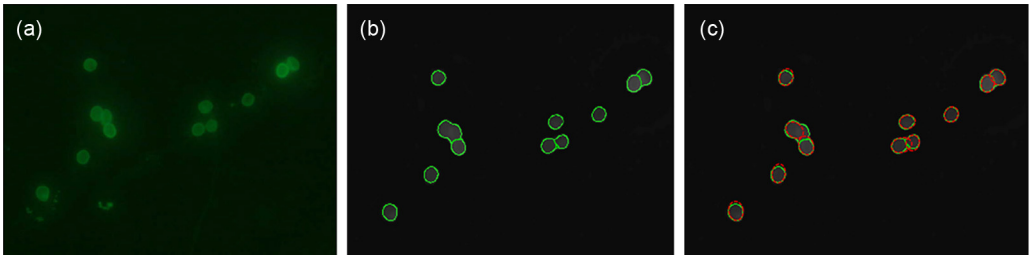

Fig. 10. Sample of *Cryptosporidium* image where parasites are not correctly detected: (a) input image, (b) detected parasite, and (c) after ellipse fitting.

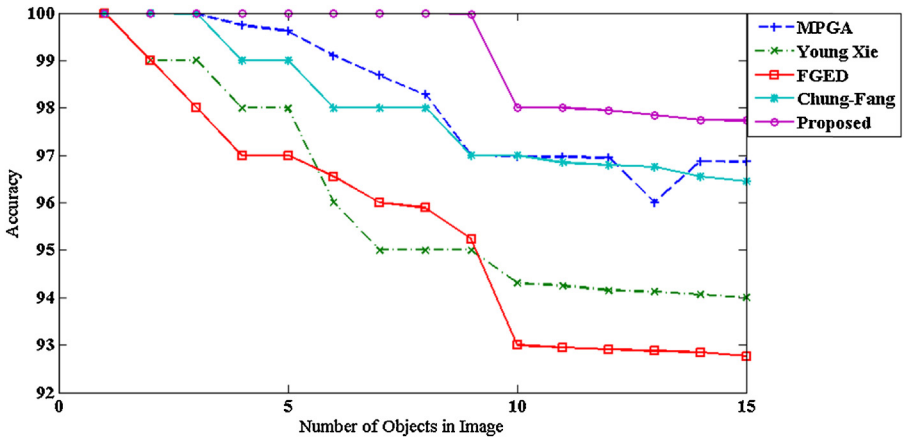

Fig. 11. Performances of the proposed and other techniques in segmenting *Cryptosporidium* oocysts.

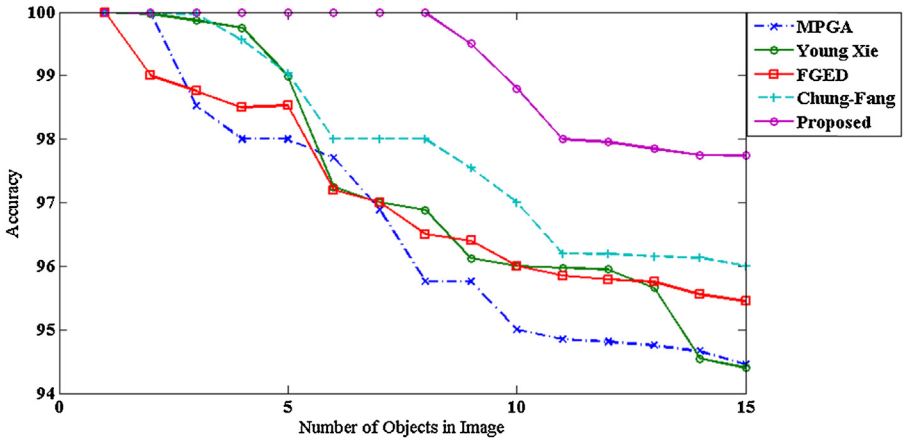

Fig. 12. Performances of the proposed and other techniques in segmenting *Giardia* cysts.

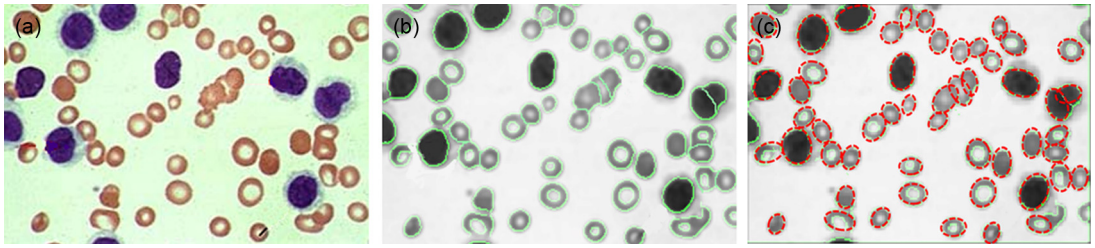

Fig. 13. Sample of blood cell image 1: (a) input image, (b) segmented image, and (c) ellipse fitting.

they can be combined into a single ellipse contour based on least square error.

The conic model used for ellipse is represented by the following equation:

$$F(x, y) = ax^2 + bxy + cy^2 + dx + ey + f = 0 \quad (13)$$

and(14)$b^2 - 4ac < 0$where a, b, c, d, e, f are coefficients of the ellipse and (x, y) are the coordinates of the pixel points on the contour. The function of Eq. (13) is called the algebraic distance of a point (x, y) to the conic $F(x, y) = 0$.

Eq. (13) can be written in vector form as

$$F_a(x) = \mathbf{x} \cdot \mathbf{a} = 0 \quad (15)$$

where $\mathbf{a} = [a, b, c, d, e, f]^T$ and $\mathbf{x} = [x^2, xy, y^2, x, y, 1]$ while T is the transpose operator.

3. Result

The platform used to implement the proposed technique is MATLAB R2013a. The performance of the proposed technique was tested on two custom databases. The first database was obtained from the Department of Parasitology, University of Malaya, and it contains 20 images of *Giardia* cysts and 20 images of *Cryptosporidium* oocysts in treated water. In each image, the number of (oo)cysts that are present varies from 1 to 15. The second database contains 15 images of overlapping blood cells, *Cryptosporidium* oocysts in dirty background and rice grains. In each image, the number of objects is from 8 to 53.

In the first database, each of the image contains solitary and overlapping (oo)cysts and there are a total of 266 (oo)cysts altogether. Using the proposed method, 262 (oo)cysts were segmented correctly which translates to 98.5% average detection rate. Fig. 6 shows examples of *Giardia* cysts before and after segmentation. In

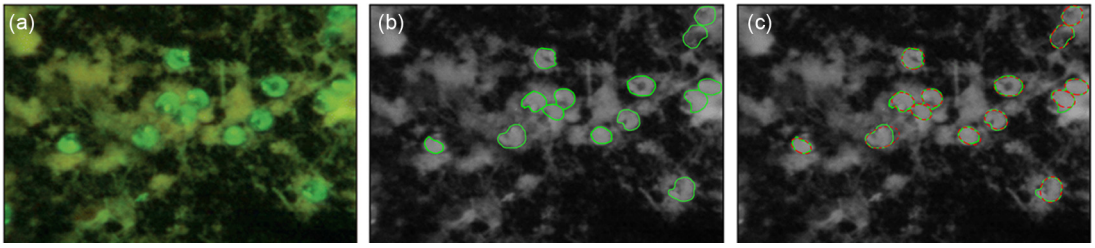

Fig. 14. Sample of (oo)cysts image 1 with noisy background: (a) input image, (b) segmented image, and (c) ellipse fitting.

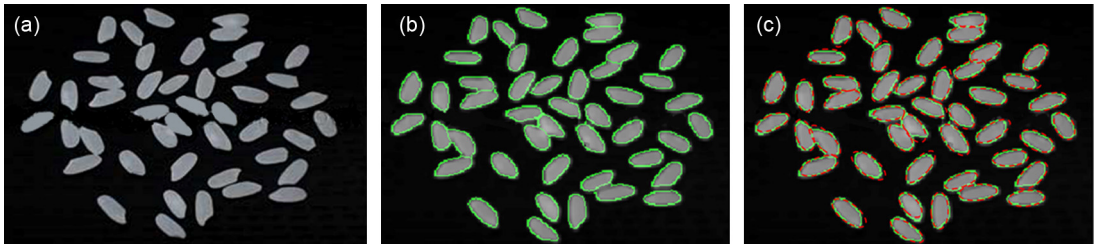

Fig. 15. Sample of rice grain image 1: (a) input image, (b) segmented image, and (c) ellipse fitting.

the figure, only the segmentation of the overlapping (oo)cysts is shown in the cropped and enlarged sub-image.

Figs. 7 and 8 show segmentation of the *Giardia* parasites which are segmented correctly and incorrectly.

Figs. 9 and 10 also show the segmentation of *Cryptosporidium* which are detected correctly and incorrectly, respectively. As observed, some of the wrongly segmented (oo)cysts have blurred boundary. Some others are significantly obscured and hidden behind other (oo)cysts. In some other cases the (oo)cysts are relatively faint and hard to observe such that they are removed as noise during filtering process.

Table 2 shows the accuracy and average execution time of the proposed technique compared to that of the others.

The performance comparison between the proposed technique and four well-known ellipse detection methods in detecting overlapping (oo)cysts is shown in Figs. 11 and 12. The four approaches are selected since they are well known and widely used by practitioners in various applications and they are Xie's algorithm [4],

Table 3
Accuracy of proposed technique on blood cell, (oo)cysts and rice grain images against other four methods.

Image category	Number of images	MPGA	Young	FGED	Chung	Proposed
Blood Cells	Image 1 *Total objects 51*	48	48	47	48	50
	Image 2 *Total objects 53*	47	46	48	48	52
	Image 3 *Total objects 35*	33	33	32	33	35
	Image 4 *Total objects 32*	30	31	30	30	32
	Image 5 *Total objects 15*	12	13	13	13	14
(oo)Cysts	Image 1 *Total objects 14*	13	10	10	12	14
	Image 2 *Total objects 14*	13	13	13	12	13
	Image 3 *Total objects 15*	13	13	13	12	14
	Image 4 *Total objects 9*	9	8	7	8	9
	Image 5 *Total objects 53*	50	49	49	50	52
Rice grain	Image 1 *Total objects 45*	43	43	40	44	45
	Image 2 *Total objects 8*	8	7	8	8	8
	Image 3 *Total objects 9*	8	8	9	8	9
	Image 4 *Total objects 37*	31	33	34	35	36
	Image 5 *Total objects 24*	23	23	22	22	24
Accuracy		92.02%	91.30%	90.57%	92.51%	98.30%

FGED algorithm by Elmowafy and Fairhurst [6], the MPGA method by Yao et al. [9], the multi-resolution Hough transform method by Chien [7].

The second database consists of images of blood cells, (oo)cysts in dirty background and rice grains in equal numbers. There are five images of each object type and altogether there are 15 images. The number of blood cells, (oo)cysts and rice grains in the images varies from 8 to 53. From each category one sample of the results are shown in Figs. 13–15. In each figure, the original image is followed by the results of contour tracing and ellipse fitting.

Table 3 presents the accuracy of the proposed technique against those of the other four methods in detecting blood cells, *Cryptosporidium* oocysts and rice grains in those images.

The robustness of the approach is tested in segmenting objects of different sizes and shapes in the 15 images of the second database. The overall average segmentation rate achieved by the proposed method is 98.3% which is slightly better than the other four approaches.

4. Conclusion

In this paper a new contour tracing technique is employed to segment and count overlapping *Cryptosporidium* and *Giardia* (oo)cysts found in microscopic images of treated water samples. The tracing algorithm traverses in clockwise and anti-clockwise directions on the contour of the (oo)cysts. The proposed technique is tested on a custom database containing 20 images of *Giardia* cysts and 20 images of *Cryptosporidium* oocysts. The effectiveness of the system is measured in terms of its ability to detect and segment solitary and overlapping (oo)cysts in the microscopic images of treated water samples. An excellent average segmentation rate of more than 98% is achieved for both parasites. The performance of the proposed technique is compared against those of existing well-known ellipse detection techniques. In most cases, the proposed technique performs as well as or better than the established techniques. The method is also tested on other images containing overlapping blood cells, *Cryptosporidium* oocysts in dirty background and rice grains, and the results are satisfactory. In the future, the method should be further tested on more images containing overlapping and partial (oo)cysts in noisy and dirty background. Furthermore, the technique should also be subjected to images containing objects with broken boundary lines and non-elliptical shape. A measure of angle information should be incorporated to identify the curve along the tracing line for more accurate identification of broken or incomplete object boundary.

Acknowledgments

This research is fully supported by High Impact Research Grant Scheme (D000016-16001) under the Ministry of Higher Education Malaysia.

References

[1] J. Illingworth, J. Kittler, The adaptive Hough transform, IEEE Trans. Pattern Anal. Mach. Intell. (1987) 690–698.
[2] D.H. Ballard, Generalizing the Hough transform to detect arbitrary shapes, Pattern Recognit. 13 (1981) 111–122.
[3] L. Xu, E. Oja, P. Kultanen, A new curve detection method: randomized Hough transform (RHT), Pattern Recognit. Lett. 11 (1990) 331–338.
[4] Y. Xie, Q. Ji, A new efficient ellipse detection method, in: Proceedings in 16th International Conference on Pattern Recognition, 2002, pp. 957–960.
[5] Z. Cheng, Y. Liu, Efficient technique for ellipse detection using restricted randomized Hough transform, in: Proceedings. International Conference on Information Technology: Coding and Computing, ITCC 2004, 2004, pp. 714–718.
[6] O. Elmowafy, M. Fairhurst, Improving ellipse detection using a fast graphical method, Electron. Lett. 35 (1999) 135–137.
[7] C.-F. Chien, Y.-C. Cheng, T.-T. Lin, Robust ellipse detection based on hierarchical image pyramid and Hough transform, J. Opt. Soc. Am. A: Opt. Image Sci. Vis. 28 (2011) 581–589.
[8] E. Lutton, P. Martinez, A genetic algorithm for the detection of 2D geometric primitives in images, in: Proceedings of the 12th IAPR International Conference on Pattern Recognition, 1994. Vol. 1 – Conference A: Computer Vision & Image Processing, 1994, pp. 526–528.
[9] J. Yao, N. Kharma, P. Grogono, A multi-population genetic algorithm for robust and fast ellipse detection, Pattern Anal. Appl. 8 (2005) 149–162.
[10] T. Mainzer, Genetic Algorithm for Shape Detection, 2002.
[11] R. Vaddi, L. Boggavarapu, H. Vankayalapati, K. Anne, Contour detection using freeman chain code and approximation methods for the real time object detection, Asian J. Comput. Sci. Inf. Technol. 1 (2013).
[12] F. Chang, C.-J. Chen, C.-J. Lu, A linear-time component-labeling algorithm using contour tracing technique, Comput. Vis. Image Underst. 93 (2004) 206–220.
[13] G. Wagenknecht, A contour tracing and coding algorithm for generating 2D contour codes from 3D classified objects, Pattern Recognit. 40 (2007) 1294–1306.
[14] J.I. Olszewska, T.L. McCluskey, Ontology-coupled active contours for dynamic video scene understanding, in: 15th IEEE International Conference on Intelligent Engineering Systems (INES), 2011, pp. 369–374.
[15] M. Lysaker, A. Lundervold, X.-C. Tai, Noise removal using fourth-order partial differential equation with applications to medical magnetic resonance images in space and time, IEEE Trans. Image Process. 12 (2003) 1579–1590.
[16] P.-S. Liao, T.-S. Chen, P.-C. Chung, A fast algorithm for multilevel thresholding, J. Inf. Sci. Eng. 17 (2001) 713–727.